An analysis of constraints on relativistic species from primordial nucleosynthesis and the cosmic microwave background

Kenneth M. Nollett*

Physics Division, Argonne National Laboratory, Argonne, IL 60439, USA

Gilbert P. Holder

Department of Physics, McGill University, Montreal, QC H3A 2T8, Canada

(Dated: December 13, 2011)

We present constraints on the number of relativistic species from a joint analysis of cosmic microwave background (CMB) fluctuations and light element abundances (helium and deuterium) compared to big bang nucleosynthesis (BBN) predictions. Our BBN calculations include updates of nuclear rates in light of recent experimental and theoretical information, with the most significant change occuring for the $d(p,\gamma)^3$He cross section. We calculate a likelihood function for BBN theory and observations that accounts for both observational errors and nuclear rate uncertainties and can be easily embedded in cosmological parameter fitting. We then demonstrate that CMB and BBN are in good agreement, suggesting that the number of relativistic species did not change between the time of BBN and the time of recombination. The level of agreement between BBN and CMB, as well as the agreement with the standard model of particle physics, depends somewhat on systematic differences among determinations of the primordial helium abundance. We demonstrate that interesting constraints can be derived combining only CMB and D/H observations with BBN theory, suggesting that an improved D/H constraint would be an extremely valuable probe of cosmology.

PACS numbers: 98.80.-k, 26.35.+c, 98.70.Vc, 14.60.St, 25.10.+s

I. INTRODUCTION

The sensitivity of early-universe cosmology to the number and properties of light particle species was recognized early in the development of the hot big bang model [1–4]. The expansion rate of the universe at early times increases with number of relativistic particle species in thermal equilibrium, and this in turn sets timescales for big bang nucleosynthesis (BBN). One can then use the BBN yields of light nuclei to constrain the number of light species quantitatively [5]. Constraints on the expansion rate are therefore often expressed in units of an effective number of light fermion species $N_{\rm eff}$, so that for the standard model of particle physics $N_{\rm eff} \sim 3$, while $N_{\rm eff} \neq 3$ corresponds to some altered expansion rate that might be caused by additional neutrino species or by some other effect (like a nonzero neutrino chemical potential or violations of general relativity) [79]. Recent BBN-derived constraints may be found in Refs. [6–8]. The cosmic microwave background (CMB) is sensitive to the expansion rate much later: at the times of equal matter and radiation densities and of hydrogen recombination. Recent measurements of the CMB power spectrum now allow interesting constraints on $N_{\rm eff}$ at those times [9–12].

Constraints on light species from BBN and the CMB have been examined many times as both observational data and theoretical calculations have improved. The consistency or not of these two types of constraints is an important question, particularly since they probe expansion rates at widely separated times in the evolution of the universe. In the present work, we check for consistency between the two data sets, examine the sensitivity of that consistency to model assumptions, and then attempt to place the strongest constraint possible on $N_{\rm eff}$ by combining the two types of data.

The BBN yields – especially of deuterium – depend not just on $N_{\rm eff}$ but also on the cosmological baryon density, which in units of the critical density of the universe is $\Omega_b \equiv 8\pi G\rho_B/3h^2$. ($h$ is the Hubble constant in units of $100 \text{ km s}^{-1} \text{ Mpc}^{-1}$, G is Newton's constant, and ρ_B is the baryon density expressed as mass per unit volume.) Prior to the precise inference of $\Omega_b h^2$ from CMB measurements, the strongest constraint on $N_{\rm eff}$ came from using the deuterium-to-hydrogen number ratio D/H to restrict $\Omega_b h^2$ and then exploiting the $N_{\rm eff}$ dependence of the primordial helium mass fraction $Y_{\rm p}$. However, D/H has its own dependence on $N_{\rm eff}$ [6, 13]; a strong external constraint on $\Omega_b h^2$ allows BBN constraints on $N_{\rm eff}$ that are independent of $Y_{\rm p}$. We show below that, particularly because precise measurements of $Y_{\rm p}$ are difficult, the constraint on $N_{\rm eff}$ from D/H is competitive with that from $Y_{\rm p}$.

In this paper, we focus on three issues: a full update of the BBN reaction rates including a revision to the $d(p,\gamma)^3$He rate based on recent theoretical calculations; an implementation of BBN constraints that includes both observational and theoretical uncertainties within CosmoMC [14] (a popular Markov chain Monte Carlo fitting program used for cosmological data); and the utility of D/H as a probe of new physics that is independent of uncertainties in the primordial helium abundance.

arXiv:1112.2683v1 [astro-ph.CO] 12 Dec 2011

II. BIG-BANG NUCLEOSYNTHESIS AND $N_{\rm eff}$

BBN constraints on physics and cosmology require accuracy in both computed BBN yields and observed abundances. With only standard-model physics (N_ν=3, no late-decaying particles, negligible neutrino chemical potentials, etc.), BBN is a one-parameter model, depending on the baryon density. Since $\Omega_b h^2 = 0.02249(55)$ [9] is now known to $\sim$ 3% from the CMB alone, this "standard" BBN is a high-precision theory with no free parameters. The predicted $Y_{\rm p}$ has a precision of $\sim$ 0.2%, while yields of D, ^{3}He, and ^{7}Li are predicted with respective precisions of roughly 5%, 4%, and 8% (computed below and e.g. in Refs.[15–19]). To constrain deviations from this standard model, we need both accurate BBN calculations based on up-to-date nuclear inputs and observationally-inferred primordial abundances.

A. The BBN calculation

We compute BBN light-nuclide yields using a modified version of the Wagoner/Kawano code described in Ref. [20]. We adjusted the timestep controls to compute yields more precisely than 0.1% for given nuclear rates, and we used the Monte Carlo techniques described in Ref. [17] to propagate nuclear cross section data into yields and yield uncertainties. For the centroid of our $Y_{\rm p}$ predictions we used the independent BBN code of Lopez and Turner [21]. It accounts for several small effects in weak-interaction physics and the equation of state and achieves a theoretical precision (for a given neutron mean lifetime τ_n) of $\Delta Y_{\rm p} < 0.0002$ or < 0.1%. The $Y_{\rm p}$ from this code has been shown to agree within this margin with somewhat independent calculations [22]. We note that its results are $\Delta Y_{\rm p} \sim 0.0004$ higher than those reported in Ref. [16] for reasons that are unclear – each calculation should have a higher precision than this. For comparison, the uncertainty arising from the currently recommended τ_n is ~ 0.0003 (but see below for its likely underestimation).

BBN codes integrate a set of coupled rate equations to evolve light-nuclide abundances in the expanding and cooling universe. The rate coefficients in those equations are in turn based on nuclear cross sections, mainly inferred from experiment. Several improvements in the nuclear inputs have occurred in the decade since the study of Ref. [17], so we have updated the input database used there accordingly. We now summarize those changes with an emphasis on the D and ^{4}He yields that are useful for constraining $N_{\rm eff}$. In addition to the reactions affecting $Y_{\rm p}$ and D/H, the input database for the reaction ^{3}He$(\alpha, \gamma)^7$Be has also been brought up to date by including recent data examined in Refs. [19, 23]; this affects only the curves shown in Fig. 2 and almost none of the discussion.

1. The reaction $p(n, \gamma)d$

There are very few cross section data for neutron capture on protons at energies relevant for BBN, though the situation has improved in recent years [24], and their precision is generally rather low. For this reason, BBN evaluations in the 1990s [17, 25] used theoretical cross sections from the ENDF/B-VI and earlier databases [26] rather than fitting the data. In general, theoretical calculations more precise than the data at BBN energies [26–28] were possible, but some calculations had only been carried out for thermal neutrons, and uncertainties were poorly quantified.

The BBN calculations of Refs. [17, 25] applied to the ENDF cross section a conservative 5% error in overall normalization that had a somewhat murky origin in the literature. It has subsequently been shown using pionless effective field theory (EFT) that the low-energy cross section can be computed from a small number of input quantities (most at least implicitly used in the ENDF cross section) and shown to have an error of < 1% at BBN energies [29, 30]. We have accordingly used the EFT results [29] to compute the rate of $p(n, \gamma)d$, assigned it an overall normalization error of 1%, and incorporated the results into the BBN code in place of the ENDF/B-VI rate. Since the EFT rate agrees with the old ENDF rate, this results in a much smaller error on D/H but does not shift the most-likely yield.

2. The reactions $d(d, n)^3$He and $d(d, p)^3$H

The investigations in Ref. [17] resulted in a call for improved data on deuteron-deuteron reactions at 100 to a few hundred keV (center-of-mass), where there were no modern data with well-quantified errors. The response was the work of Ref. [31], which produced data with a precision of $\sim$ 2%. We added these results to our rate database along with lower-energy data [32] that were missed in the literature search of Ref. [17]. The addition of these data reduces the error on D/H, particularly at low values of $\Omega_b h^2$ where $d + d$ reactions formerly dominated the error budget [17]. The new data shift D/H by less than 1% relative to previous results [17, 33].

3. The reaction $d(p, \gamma)^3$He

It was found in Ref. [17] and by other authors [15, 34, 35] that the only reactions important for the uncertainty on the D/H yield were the three reactions discussed above and proton capture on deuterium. Even before the above updates to $p(n, \gamma)d$ and $d + d$ rates, the $d(p, \gamma)^3$He rate dominated the error on D/H at the CMB-inferred $\Omega_b h^2$.

The effect of using measured $d(p, \gamma)^3$He cross sections in BBN calculations has not changed since our previous study Ref. [17]. There has been one published low-energy cross section measurement since then [36], and we have

updated our database to include it. As the new data are well below most of the BBN energy window shown in Fig. 1, and they agree with previous data there, they do not affect our results discernably. This calculation will be referred to as "Empirical dpγ" below.

Fig. 1 shows the scarcity of laboratory data for this reaction at BBN energies that was cited in Ref. [17] as a cause for concern in both rate determination and error estimation. Cross section fitting for charged-particle reactions is generally done with s-wave Coulomb barrier penetration divided out, in terms of the S-factor

$$S(E) = E e^{2\pi Z_1 Z_2 \alpha c/v} \sigma(E),$$

where σ is the cross section, E the energy, Z_i the nuclear charges, α the fine-structure constant, c the speed of light, and v the relative velocity. Except for one rate evaluation using the R-matrix formalism [37], all BBN work to date has fitted $S(E)$ either as a polynomial with poor physical motivation [15, 16, 25] or as an expansion in linearly-independent, locally-supported B-splines [17] in which $S(E)$ at a given energy is determined by nearby data. There is only one modern data set for $d(p,\gamma)^3$He at the most important energy range of 50 – 500 keV [38], so only the R-matrix approach allows independent measurements to average against it in a physically motivated way.

Because ab $initio$ nuclear theory is now quite accurate for many bound-state and continuum properties of three-body systems [41], a purely empirical approach to $d(p,\gamma)^3$He is no longer required; the situation with $d(p,\gamma)^3$He is now similar to that with $p(n,\gamma)d$. In particular, the Pisa group has computed the cross section of $d(p,\gamma)^3$He using accurate two- and three-nucleon potentials, corresponding two- and three-body corrections to the electromagnetic currents, and accurate methods of solution [39, 40]. The results are in very good agreement with data above and below the BBN energy range (particularly the new low-energy data of Ref. [36]), not only in total cross section but also in angular-distribution and polarization observables. However, the total cross section is well above most of the sparse data at BBN energies.

The energy dependence of the cross section is determined by competition between s- and p-wave capture, which is probed by the polarization observables. Since both they and the low-energy total cross sections support the model, we suspect that the data of Ref. [38] may have a systematically low normalization by about 20% (compared with their stated systematic error of 9%) and that the theoretical curve provides a better guide to the actual cross section.

For these reasons, we adopt the ab $initio$ cross section [39, 40] for our BBN calculations. The precision of the calculation is likely a few percent at worst, but it is difficult to determine. Errors could in principle be propagated through the constraints on "model-dependent" two-body currents, but these are themselves small corrections to the main two-body corrections that make up $\sim 15\%$ of the cross section. The remaining errors arise
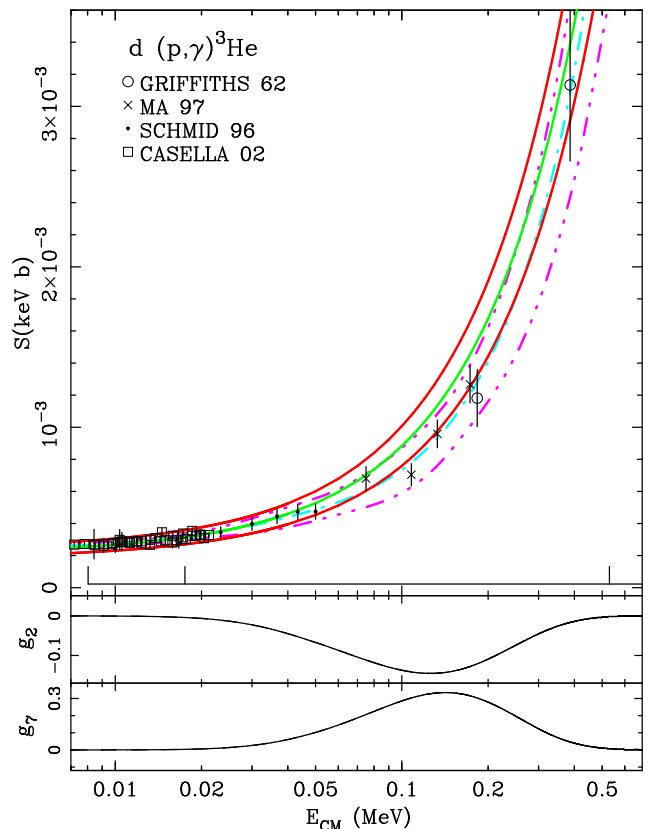

FIG. 1: (Color online) Upper Panel: S-factor data for the reaction $d(p,\gamma)^3$He are shown, along with the best-fit curve and 2σ intervals based purely on those data [17] (dash-dot and dash-dot-dot-dot curves) and on the ab $initio$ calculation [39, 40] (solid). All errors are shown as 2σ intervals for comparability with Fig. 3 of Ref. [17]. Lower Panels: Sensitivity functions [17] showing the relative importance of this reaction at varying energy for D/H (g_2) and Li/H (g_7) yields, evaluated at $\Omega_b h^2 = 0.019$. Convolving the S-factor error band with the sensitivity function gives the total uncertainty arising from this reaction. The strongest sensitivity to the $d(p,\gamma)^3$He rate occurs at the largest $|g_i|$, in the 50–500 keV range.

from the numerical method of computation (probably negligible) and the nuclear interaction model. The methods that have been used to construct the modern nucleon-nucleon potentials (~ 40 parameters fitted to thousands of data points from many experiments) have not been adapted to facilitate error propagation. The modern potentials do reproduce many properties of two- and three-nucleon systems [28, 41, 42] at the percent level, and they have also been applied very successfully to larger systems (e.g., [43]).

Because assigning a quantitative error to the computed cross section is difficult, we would like to be conservative. The case of $p(n,\gamma)d$ is again analogous: through the 1990s, errors of 5% were assigned to an evaluation that later proved accurate to something more like 1% [17, 25]. The review of Ref. [23] presents a polynomial

fit to the $d(p,\gamma)^3$He S-factor and a recommended cross section primarily for use well below the BBN range. This fit's normalization is dominated by the precise and copious low-energy data, which cause the recommended $S(0)$ to have an error of 7%. The *ab initio* cross section is in essentially perfect agreement with the low-energy data, so we adopt 7% as the precision to which it has been tested and apply this as an overall error on its normalization. This error is handled in our BBN Monte Carlo procedure just like that for the $p(n,\gamma)d$ cross section. Ref. [17] in effect propagated a 9% error bar from the nuclear data, so adopting 7% does not drastically change the (dominant) contribution of $d(p,\gamma)^3$He to the yield errors. We use these results rather than the "Empirical dpγ" calculation described above in our likelihood analysis.

The larger *ab initio* cross section for $d(p,\gamma)^3$He at BBN energies results in more destruction of deuterium at late times than was found previously [17, 44]. At the WMAP baryon density [9], this amounts to about a 5.6% reduction of D/H; the D/H-inferred $\Omega_b h^2$ is shifted downward by roughly half a standard deviation. In light of the severity of this shift, independent cross section measurements at 50–500 keV would be quite useful. The shift in the $d(p,\gamma)^3$He rate also increases the ^{7}Li yield by about 10% through its effect on the availability of ^{3}He at late times, worsening slightly the primordial ^{7}Li problem reviewed in Ref. [45].

4. The neutron lifetime τ_n

The mean lifetime τ_n of the neutron is used in the BBN calculation to normalize all of the weak-interaction rates that interconvert neutrons and protons at early times. It may be conveniently thought of as determining the weak coupling constant G_F, and its uncertainties propagate through the weak rates into the abundance yields.

The work of Refs. [17, 21] used a neutron mean lifetime of $\tau_n = 885.4 \pm 2.0$ s, which was the most recent experimental result at the time. This result was subsequently included in the world average of 885.7 ± 0.8 s recommended for several years by the Particle Data Group [46]. More recently, conflicting lifetimes of $878.5 \pm 0.7 \pm 0.3$ s and $880.7 \pm 1.3 \pm 1.2$ s have been reported respectively by Serebrov et al. [47, 48] and Pichlmaier et al. [49]. The Particle Data Group now recommends a world average that includes conflicting values, 881.5 ± 1.5 s [50], with errors that have been inflated to reflect the discrepancy.

We performed our calculations using the currently recommended τ_n with its recommended error, and these form the basis of our reported results. We also performed BBN calculations with the formerly recommended $\tau_n = 885.7 \pm 0.8$ s and with $\tau_n = 878.5 \pm 1$ s from Serebrov. The difference between the two amounts to $\Delta Y_{\rm p} \simeq 0.0015$, equivalent to $\Delta N_{\rm eff} \simeq 0.12$. The effect on D/H is a shift of 0.4% at $\Omega_b h^2 = 0.0225$. For both yields, the difference is much smaller than the other uncertainties in our analysis.

B. The $N_{\rm eff}$ dependences of D/H and $Y_{\rm p}$

We computed BBN yields, including their errors and correlation coefficients, on a grid covering $\Omega_b h^2$ from 0.005 to 0.1 and $N_{\rm eff}$ from 0.046 to 10.046. This includes the entire range sampled in our Markov chain Monte Carlo (MCMC) analysis below, allowing considerable margins at the edge of the grid. We show all BBN yields as functions of $\Omega_b h^2$ over this grid in the left panels of Fig. 2. Separate curves are shown, with widths indicating 1σ errors, at integer intervals in $N_{\rm eff}$. This indicates the nature and strength of the sensitivity to $N_{\rm eff}$. The dependence of $Y_{\rm p}$ and D/H on $N_{\rm eff}$ is apparent; that of $Y_{\rm p}$ is much larger, relative to its yield uncertainties, than that of D/H. At the band indicating the current WMAP value of $\Omega_b h^2$, D/H changes by about 10% per unit $N_{\rm eff}$.

The right side of Fig. 2 shows the dependences of BBN yields on $N_{\rm eff}$ and on the assumed rates of $d(p,\gamma)^3$He and of the weak processes scaled by τ_n. Each yield was computed at $\Omega_b h^2 = 0.02260(54)$, inferred below from a cosmological analysis of CMB fluctuations marginalized over $Y_{\rm p}$ and $N_{\rm eff}$, and the error on $\Omega_b h^2$ was added in quadrature to the nuclear uncertainties. The diagonal curves are thus essentially slices along the "WMAP" band in the left panels of Fig. 2. The effects on D/H and ^{7}Li/H of switching $d(p,\gamma)^3$He rates are shown as black curves with no error band in the right side of Fig. 2; that on D/H corresponds roughly to $\Delta N_{\rm eff} = 0.42$. Similarly, the effects of assuming either the pre-2011 or the Serebrov values of τ_n are shown as black curves without error bands next to the $Y_{\rm p}$ yield curve. To a very good approximation, $d(p,\gamma)^3$He does not affect $Y_{\rm p}$ and τ_n does not affect D/H.

The yields $Y_{\rm p}$ and D/H measure slightly different things [5]. At the start of standard BBN the population of relativistic particles consists of photons, electrons, positrons, and three species of neutrinos, all at the same temperature. At a given temperature, the resulting expansion rate of the universe is 2.3 times that from photons alone. Weak freezeout begins at this time, setting the neutron/proton ratio that will eventually determine $Y_{\rm p}$. An additional neutrino species speeds the expansion rate by $\sim 40.3\%$, so that weak freezeout occurs at higher temperature. Higher temperature at equilibrium implies more neutrons, so faster expansion yields more ^{4}He.

In contrast, the abundance of deuterium is determined by $d + d$ and $d + p$ reactions toward the end of BBN, when the photon temperature is well below the electron rest mass. At these times, there are essentially no electrons or positrons, and the energy they previously carried has been transferred to the photons, which are consequently at higher temperature than the neutrinos. The expansion rate at this time in standard BBN is ~ 1.7 times that of photons alone, so that adding a neutrino species at the same temperature as the others causes a $\sim 36.7\%$ speed-up. Faster expansion implies less time available for deuterium burning and thus higher D/H. In the standard model, deuterium burning and the recom-
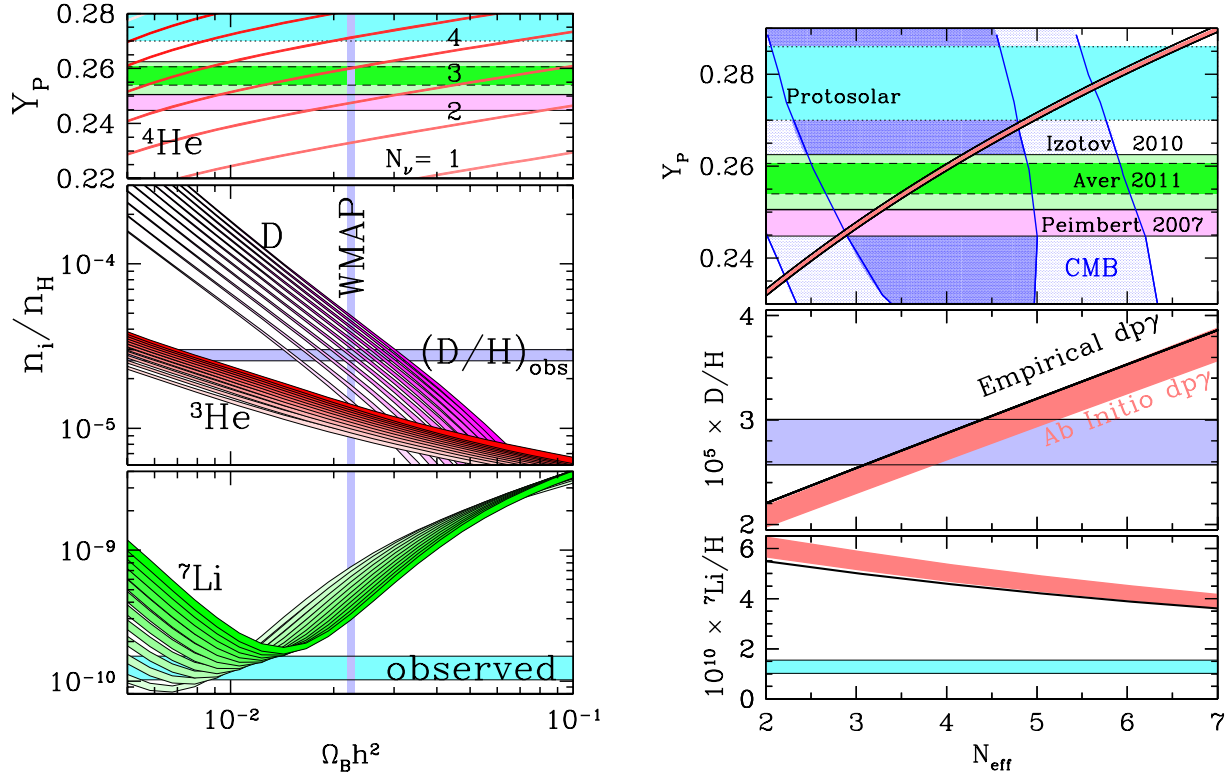
FIG. 2: (Color online) Left panels: Yields of light nuclides as functions of the baryon density, $\Omega_b h^2$. Each band indicates yields for a single value (integer plus 0.046) of $N_{\rm eff}$ and its thickness the 1σ nuclear uncertainty on those yields. Bands are shaded lighter for smaller values of $N_{\rm eff}$ and darker for larger $N_{\rm eff}$. Also shown are horizontal bands indicating observational constraints on abundances [51–55] and a vertical band indicating the WMAP7 1σ interval for $\Omega_b h^2$. Right panels: The same yields shown as functions of $N_{\rm eff}$ at the CMB-inferred value of $\Omega_b h^2$, essentially slices along the band labeled "WMAP" in the left panels. Salmon-colored bands indicate yields with our adopted rates, and their widths indicate a quadrature sum of nuclear errors and the error on $\Omega_b h^2$. In the $Y_{\rm p}$ graph, blue 1σ and 2σ contours indicate constraints from WMAP7+SPT alone, while black curves paralleling the adopted yields indicate the effects of using the old Particle Data Group [46] (upper) and Serebrov [48] (lower) values of τ_n (no errors shown). In the D/H and ^{7}Li/H graphs, the thin solid curves indicate the result of using the empirical rate for $d(p,\gamma)^3$He, again without showing the errors. Horizontal bands indicate observational constraints as discussed in the text.

bination era share the same populations of relativistic species: photons plus three neutrino species at $(4/11)^{1/3}$ of the photon temperature.

C. Observed primordial abundances

Constraints based on BBN require observed abundances. The inference of each primordial abundance is a highly technical subject unto itself with its own extensive literature. Here we provide brief descriptions of the experimental constraints and explain the specific values that we choose. The interested reader is referred to the cited literature for more information, and to the reviews in Refs. [6, 45, 50, 56–58].

1. ^4He

The primordial ^{4}He mass fraction $Y_{\rm p}$ is inferred from emission-line spectra of H II regions in metal-poor blue compact galaxies. Lines of H and He are observed and a He/H ratio inferred using a radiative transfer model; the result is customarily expressed in terms of $Y_{\rm p}$. Because of the weak dependence of $Y_{\rm p}$ on $\Omega_b h^2$ evident in Fig. 2, the desired precision of measurement is in the percent range. Large data sets have been assembled, and the errors on $Y_{\rm p}$ are dominated by systematic effects in the analysis, not statistics.

A recent revision of the atomic data used to infer $Y_{\rm p}$ [59] resulted in a systematic upward shift of all data sets (but not all individual data). Three groups have published $Y_{\rm p}$ values based on the new emissivities, and we mention only the most recent publication from each. Pe-

imbert et al. [51] find 0.2477 ± 0.0029 from 5 HII regions using radiative-transfer models tailored to each object and taking into account temperature fluctuations within each HII region. Applying approaches in which physical parameters for each HII region are determined in a simultaneous fit and errors are computed by Monte Carlo, Izotov & Thuan find $0.2565 \pm 0.0010\,(\text{stat}) \pm 0.0050\,(\text{syst})$ from 93 HII regions [54] while Aver et al. find 0.2573 ± 0.0033 [55] for nine selected low-metallicity objects from the Izotov & Thuan data set.

The quoted Y_p is generally an extrapolation to zero metallicity Z of the helium mass fractions Y observed in objects of (small) nonzero Z. Peimbert et al. applied a dY/dZ slope calibrated elsewhere; Izotov & Thuan determined dY/dZ internally to their data by linear regression; the Aver et al. result quoted above is the mean of their nine selected objects, with zero slope assumed. They also derived from linear regression with no prior on dY/dZ a result of 0.2609 ± 0.0117, but it appears that their narrow metallicity range does not allow a slope to be determined. The upper end of this error interval is close to the initial Pop I composition of the Sun, $Y_{\text{proto}} = 0.278 \pm 0.008$ [60], which must be greater than Y_p since stars are net creators of ^{4}He. We repeat our analysis for each of these three input Y_p constraints.

2. ^2H

Primordial deuterium is observed in gas of very low metallicity along our lines of sight to distant quasars. Quasar light is absorbed by atomic transitions of neutral hydrogen, and deuterium is observed as additional absorption with the appropriate isotope shift and doppler width to be deuterium in the same physical location. Quasar spectra that are suitable for inference of D/H are rare, because the quasar continuum emission must be well-characterized, there must be no other absorption nearby in redshift/velocity space, and the absorber must have sufficient hydrogen column density to produce measurable absorption from its small amount of deuterium. To date there are eight extragalactic systems in which D/H is generally agreed to have been measured. These are described in Refs. [53, 61] (and references therein), where the average $\log(\text{D/H}) = -4.556 \pm 0.034$ is found. As discussed in Refs. [53, 62, 63], it is not clear that all eight systems have consistent inferred D/H. We adopt this average as the observed primordial D/H.

3. ^3He and ^7Li

The other two nuclides predicted in measurable quantities by BBN are ^{3}He and ^{7}Li. ^{3}He has only been observed in our galaxy (in HII regions) and only at relatively high metallicity [64]. Moreover, its post-BBN history is complicated, as it seems to be produced copiously in some stars but mostly burned up in oth-

ers [65]. Although its observed abundance is generally consistent with BBN, further inferences from ^{3}He seem unwarranted. The primordial ^{7}Li/H has been identified with the nearly-uniform abundance found in atmospheres of low-metallicity main-sequence turnoff stars of the Galactic halo [45, 52, 66, 67]. As shown in the left side of Fig. 2, this abundance is near the minimum producible by standard BBN at any Ω_b and a factor of 3.5 below that predicted by the WMAP Ω_b. Whether this is a consequence of post-BBN processing (most likely in the observed stars themselves) or of something missing in standard BBN is unclear [45]. Since we are considering only standard BBN apart from variation of N_{eff}, the important fact here is that even at $N_{\text{eff}} = 10$, BBN overproduces ^{7}Li by a factor of 2 relative to halo stars. Thus, it is an implicit assumption of our model that the observed Li/H is not primordial, and we do not include it in our constraints.

III. BBN AND CMB LIKELIHOOD FUNCTIONS

The cosmic microwave background is affected by extra radiation in two ways [12, 68]. On large scales the CMB is sensitive to the gravitational effect of the perturbations in the extra radiation, while on smaller scales the increased expansion rate leads to an increased amount of diffusion damping. However, changing the helium abundance also affects diffusion damping, as Y_p affects the number of electrons per unit baryon mass. The recent results of Keisler et al. [11] used CMB power spectra from the WMAP seven-year data release (WMAP7) and the South Pole Telescope (SPT) to find $N_{\text{eff}} = 3.85 \pm 0.62$ when the relation between Y_p and N_{eff} from BBN theory was enforced, ignoring uncertainties in the BBN rates. Without an imposed BBN prior on Y_p the precision of the N_{eff} measurement is degraded to $N_{\text{eff}} = 3.4 \pm 1.0$. Following Keisler et al. [11], we use bandpowers from WMAP7 and SPT, which together cover the multipole range $\ell = 2 - 3000$.

To combine BBN constraints with CMB measurements, we adopt a Markov Chain Monte Carlo (MCMC) approach, using a modified version of the publicly available package CosmoMC [14]. MCMC methods work by sampling the parameter space at random positions and either accepting or rejecting each sample based on the likelihood of that particular point in the parameter space. The most-likely values and confidence intervals for the parameters are identified from the distribution of samples.

For CMB measurements, we assume an 8-parameter spatially flat ΛCDM cosmology, allowing as parameters the cold dark matter density ($\Omega_c h^2$), the baryon density ($\Omega_b h^2$), the angular size of the sound horizon (θ_s), the optical depth to Thomson scattering in the reionized universe (τ), the amplitude (A_s, using as a parameter $\ln A_s$) and spectral index of the potential fluctuations (n_s), the helium abundance (Y_p) and the effective num-

ber of neutrino species (N_{eff}). As additional parameters, we allowed for a contribution to the SPT power from the Sunyaev-Zeldovich effect, clustered galaxies, and shot noise from galaxies, using priors from Shirokoff et al. [69], as described in Keisler et al. [11]. We assume broad uniform priors that extend well beyond the WMAP7-allowed range on all cosmological parameters and explore $0 < Y_{\text{p}} < 1$ and $1.046 < N_{\text{eff}} < 8.046$.

The BBN likelihood only depends on a small subset of these parameters: $\Omega_b h^2$, N_{eff}, and Y_{p}. For a given assumed pair of $\Omega_b h^2$ and N_{eff}, a probability distribution based on nuclear uncertainties can be calculated for Y_{p} and D/H from BBN theory. This can be multiplied by the observed joint probability distribution describing Y_{p} and D/H observations, and the resulting distribution can then be integrated over D/H to yield a final $P(Y_{\text{p}})$:

$$P(Y_{\text{p}}, D/H, N_{\text{eff}}, \Omega_b h^2 | Y_{\text{p}_{obs}}, D/H_{obs}) \propto$$
$$P(Y_{\text{p}_{obs}}, D/H_{obs} | Y_{\text{p}}, D/H)$$
$$\times P(Y_{\text{p}}, D/H | N_{\text{eff}}, \Omega_b h^2) \quad (1)$$

As written, the two factors on the right side of the equation are the observed abundances and the theory prediction for the abundances, each of which is a 2-D probability distribution.

The D/H ratio does not affect CMB observables, so we marginalize over it to obtain the final likelihood:

$$P(Y_{\text{p}}, N_{\text{eff}}, \Omega_b h^2) \propto \int P(Y_{\text{p}}, D/H, N_{\text{eff}}, \Omega_b h^2) d(D/H) \quad (2)$$

In general, this procedure could be time-consuming in a MCMC, where likelihood evaluations may be done hundreds of thousands of times. We approximate the observed and theory abundances as 2D Gaussians, with the observed abundances uncorrelated and the (small) theory covariances extracted from the Monte Carlo BBN calculations described above. In this case, Eq. (1) is simply the product of two Gaussians, the result of which is another Gaussian distribution, and the marginalization is trivial. Therefore, the likelihood evaluation and marginalization over the true D/H are reduced to an algebraic equation involving the means and covariances of the observed and theory abundances.

In more detail, following the notation of Ahrendt [70], if the probability distributions of the theoretical and observational abundances are given by multivariate normalized normal distributions $N(\vec{\mu}_{th}, \Sigma_{th})$ and $N(\vec{\mu}_{obs}, \Sigma_{obs})$, with means denoted by $\vec{\mu}$ and covariance matrices Σ, the product of these two distributions is

$$N(\vec{\mu}_{th}, \Sigma_{th}) N(\vec{\mu}_{obs}, \Sigma_{obs}) = z_c N(\vec{\mu}_{comb}, \Sigma_{comb}) \quad (3)$$

where the combined covariance matrix is

$$\Sigma_{comb} = (\Sigma_{th}^{-1} + \Sigma_{obs}^{-1})^{-1} \quad (4)$$

and the combined mean is

$$\vec{\mu}_{comb} = \Sigma_{comb}(\Sigma_{th}^{-1}\vec{\mu}_{th} + \Sigma_{obs}^{-1}\vec{\mu}_{obs}). \quad (5)$$

The prefactor is given by

$$z_c = \frac{1}{|2\pi(\Sigma_{th} + \Sigma_{obs})|^{-1/2}} \times \quad (6)$$
$$\exp\left[-\frac{1}{2}(\vec{\mu}_{th} - \vec{\mu}_{obs})^T (\Sigma_{th} + \Sigma_{obs})^{-1} (\vec{\mu}_{th} - \vec{\mu}_{obs})\right].$$

Marginalizing over D/H is then done by an analytic integral which leads to the 2-D normal distribution in Equation (3) being simply replaced by a 1-D normal distribution involving only the mean and covariance of Y_{p}.

In summary, to include full BBN information within an MCMC, one must simply supply observed He and D abundances and a covariance matrix for the observations (presumably always diagonal), and a grid of BBN predictions as functions of $\Omega_b h^2$ and N_{eff} for He and D abundances with the theoretical uncertainty expressed as a covariance matrix. While not pursued here, the generalization to include other abundances (such as ^{3}He or ^{7}Li) is straightforward in this framework.

IV. BBN AND CMB CONSTRAINTS ON N_{eff}

Before combining BBN and CMB constraints, it is important to first check for consistency. CMB-only constraints on N_{eff} marginalized over cosmological parameters and Y_{p} are weak but still useful, as can be seen in Fig. 2 and Table I (and more fully in Fig. 12 of Ref. [11]). Furthermore, we can use measurements of helium abundances to improve the precision of the CMB measurement. This is true even with weak constraints on Y_{p}, which can be provided by the protosolar abundance as an upper limit.

A lower limit on Y_{p} has less impact but also helps. It has long been recognized that observed helium abundances everywhere are too large to be attributed to stars [71]. Both observations and models of chemical evolution find $\Delta Y/\Delta Z$ in the range 1 to 5 [72] at low metallicities and smaller slopes at higher metallicities where type Ia supernovae contribute to Z. A solar metallicity of 0.014 [73], would then imply that stars have contributed at most $\Delta Y \sim 0.07$. Since $Y_{\text{proto}} = 0.278 \pm 0.008$ is the protosolar abundance, this implies $Y_{\text{p}} \gtrsim 0.22$, consistent with all observations over a long period of time (cf. Table 1 of Ref. [74] and the accompanying discussion).

Applying the weak prior that $0.22 < Y_{\text{p}} < Y_{\text{proto}}$, the precision of the CMB measurement of N_{eff} is improved to 3.87 ± 0.81. This is only slightly weaker than constraints on N_{eff} using CMB data combined with the substantially more precise measurements of Y_{p} from nearby galaxies, which are shown as the first column in Table I.

Separately, the more precise determinations of Y_{p} can be combined with D/H measurements and BBN theory to get a BBN-only measurement of N_{eff} (and a simultaneously-fit $\Omega_b h^2$ that agrees with the CMB), shown in the last column in Table I. The constraints are formally quite strong, at $\Delta N_{\text{eff}} \sim 0.25$, but results using

different Y_p determinations inherit the sometimes $> 2\sigma$ disagreement of the underlying Y_p.

A direct comparison of the first and last data columns provides a non-trivial test of cosmology. For the two higher Y_p determinations, the separate N_eff values from BBN and the CMB are in excellent agreement, suggesting that the effective number of neutrino species was the same in the first few minutes of the early universe as it was at $\sim 300\,000$ years. The lower Y_p measurement of Peimbert is in mild tension with this interpretation, with only a very slight preference for an extra neutrino species at late times but better agreement with the expectation that $N_\mathrm{eff} = 3.046$.

Given the apparent consistency, it is reasonable to combine CMB and BBN constraints. Simply requiring that the relation between Y_p and N_eff be consistent with standard BBN theory leads to an improvement in the CMB measurement, and further combining this constraint with observed light element abundances leads to the very tight constraints shown in the second and third data columns. Again, the systematically different Y_p determinations lead to challenges in interpretation: the combined analysis yields either a clear detection of an excess of effective neutrinos over the standard value of 3.046 (at $2.2 - 3.4\sigma$) or excellent agreement (within 1σ).

Given the disagreement between Y_p determinations, it is interesting that a constraint on N_eff can be obtained using CMB measurements, BBN theory, and only the D/H abundance, as can be seen in Figure 3. Using no Y_p measurements at all, there is a hint of excess radiation (at just below 2σ). This is interesting, as the current measurement of D/H is at the 10% level. It is challenging to find systems that are well-suited for this measurement, but it is not inconceivable that the D/H abundance measurement could be sustantially improved. D/H has long been viewed mainly as a probe of $\Omega_b h^2$, but it may have a future as a probe of the expansion rate encoded by N_eff with independent systematics, separate from Y_p.

V. CONCLUSION

In this paper, we have presented a comparison of determinations of the effective number of neutrino species, N_eff, from recent CMB measurements (WMAP7 and SPT) and BBN calculations, applying observed abundances of helium and deuterium in several ways. Our results are similar to those of other analyses in the recent literature [10, 75–77], though comparison is difficult because of the use of different cosmological data and model spaces and the common practice of setting $Y_p = 0.24$, which seems on the basis of Fig. 2 to bias N_eff a bit high. Like these and previous analyses, ours generally favor $N_\mathrm{eff} > 3$. The most directly comparable result in the literature combines BBN and CMB data with constraints on large-scale structure and the Hubble constant to find 95% confidence limits of $N_\mathrm{eff} = 3.90^{+0.39}_{-0.56}$ [10]. This is similar to our results.
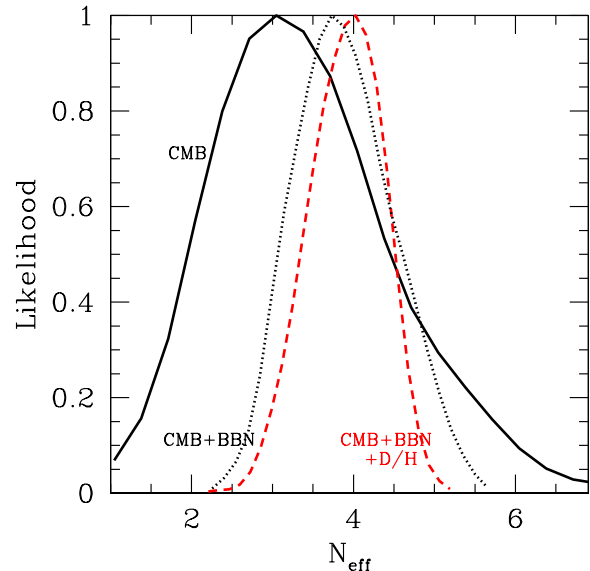

FIG. 3: (Color online) Constraints on N_eff from just CMB and D/H measurements, shown as marginalized likelihoods. The black solid curve is CMB alone, the black dotted curve shows CMB with BBN constraints on the relation between Y_p and N_eff, and the red dashed curve also adds the observed abundance of D/H.

The BBN calculation used here includes a new estimate of a key cross section, $d(p,\gamma)^3\mathrm{He}$, based on detailed new theoretical calculations, which shifts deuterium yields by $\sim 6\%$ and lithium yields by $\sim 10\%$. This new cross section shifts $\Omega_b h^2$ or Y_p inferred from D/H and slightly aggravates the large discrepancy between standard BBN and observed $^7\mathrm{Li}$ abundances.

The BBN calculations and observed abundances have been embedded in a module that can be used in a widely used MCMC code (CosmoMC) and combined with CMB measurements or other cosmological data. The BBN likelihood calculation includes both theoretical and observational uncertainties, including the weak correlation between computed D/H and Y_p.

We found that there is good agreement between BBN-based and CMB-based determinations of N_eff. These tests probe two very different epochs of the universe (a few minutes versus a few hundred thousand years), providing evidence that the same cosmological model describes both epochs. However, both probes show hints of new physics in that the preferred number of effective neutrino species is above the standard model expectation. This is especially true in the case of the two higher Y_p determinations used (based on overlapping data), with as much as a 3.4σ excess.

Setting aside the helium constraints and combining the CMB with BBN theory and the observed D/H, the excess is 2σ, at $N_\mathrm{eff} = 3.9 \pm 0.44$. Improvements in the

measurement of the D/H abundance would be extremely valuable as both a cosmological probe and an external check on Y_p determinations.

The results here underscore the complementarity of CMB measurements, BBN theory, and light element abundance measurements. CMB measurements allow both an increased precision in BBN predictions (through a robust measurement of the baryon density) and a strong test for BBN (through comparisons with N_{eff} and Y_p determinations). This is a consequence of the strong linkages in the standard cosmology between light element yields in the early universe and observable signatures at recombination, which connect the underlying cosmological model, the acoustic oscillations and Silk damping observed in the CMB, and the abundances observed in low-metallicity systems. Precise measurements of all of these interlocking observables provide strong tests of the model and its parameters.

[1] C. Hayashi, Progress of Theoretical Physics **5**, 224 (1950).
[2] R. A. Alpher, J. W. Follin, and R. C. Herman, Physical Review **92**, 1347 (1953).
[3] P. J. Peebles, Physical Review Letters **16**, 410 (1966).
[4] V. F. Shvartsman, Soviet Journal of Experimental and Theoretical Physics Letters **9**, 184 (1969).
[5] G. Steigman, D. N. Schramm, and J. E. Gunn, Physics Letters B **66**, 202 (1977).
[6] G. Steigman, J. Cosmo. Astropart. Phys. **4**, 29 (2010), arXiv:1002.3604.
[7] J. Hamann, S. Hannestad, G. G. Raffelt, I. Tamborra, and Y. Y. Y. Wong, Physical Review Letters **105**, 181301 (2010), arXiv:1006.5276.
[8] G. Mangano and P. D. Serpico, Physics Letters B **701**, 296 (2011), arXiv:1103.1261.
[9] E. Komatsu, K. M. Smith, J. Dunkley, C. L. Bennett, B. Gold, G. Hinshaw, N. Jarosik, D. Larson, M. R. Nolta, L. Page, et al., Astrophys. J. Suppl. **192**, 18 (2011), arXiv:1001.4538.
[10] J. Hamann, S. Hannestad, G. G. Raffelt, and Y. Y. Y. Wong, J. Cosmo. Astropart. Phys. **9**, 34 (2011), arXiv:1108.4136.
[11] R. Keisler, C. L. Reichardt, K. A. Aird, B. A. Benson, L. E. Bleem, J. E. Carlstrom, C. L. Chang, H. M. Cho, T. M. Crawford, A. T. Crites, et al., Astrophys. J. **743**, 28 (2011), arXiv:1105.3182.
[12] Z. Hou, R. Keisler, L. Knox, M. Millea, and C. Reichardt, ArXiv e-prints (2011), arXiv:1104.2333.
[13] C. Y. Cardall and G. M. Fuller, Astrophys. J. **472**, 435 (1996), arXiv:astro-ph/9603071.
[14] A. Lewis and S. Bridle, Phys. Rev. D **66**, 103511 (2002).
[15] R. H. Cyburt, Phys. Rev. D **70**, 023505 (2004), arXiv:astro-ph/0401091.
[16] P. D. Serpico, S. Esposito, F. Iocco, G. Mangano, G. Miele, and O. Pisanti, J. Cosmo. Astropart. Phys. **12**, 10 (2004), arXiv:astro-ph/0408076.
[17] K. M. Nollett and S. Burles, Phys. Rev. D **61**, 123505 (2000), arXiv:astro-ph/0001440.
[18] A. Coc, E. Vangioni-Flam, P. Descouvemont, A. Adah-

chour, and C. Angulo, Astrophys. J. **600**, 544 (2004), arXiv:astro-ph/0309480.
[19] R. H. Cyburt, B. D. Fields, and K. A. Olive, Journal of Cosmology and Astro-Particle Physics **11**, 12 (2008), arXiv:0808.2818.
[20] L. H. Kawano, *Fermilab-pub-92/04-a* (1992), (unpublished).
[21] R. E. Lopez and M. S. Turner, Phys. Rev. D **59**, 103502 (1999), arXiv:astro-ph/9807279.
[22] K. A. Olive, G. Steigman, and T. P. Walker, Phys. Rep. **333**, 389 (2000), arXiv:astro-ph/9905320.
[23] E. G. Adelberger, A. García, R. G. H. Robertson, K. A. Snover, A. B. Balantekin, K. Heeger, M. J. Ramsey-Musolf, D. Bemmerer, A. Junghans, C. A. Bertulani, et al., Reviews of Modern Physics **83**, 195 (2011), arXiv:1004.2318.
[24] K. Y. Hara, H. Utsunomiya, S. Goko, H. Akimune, T. Yamagata, M. Ohta, H. Toyokawa, K. Kudo, A. Uritani, Y. Shibata, et al., Phys. Rev. D **68**, 072001 (2003).
[25] M. S. Smith, L. H. Kawano, and R. A. Malaney, Astrophys. J. Suppl. **85**, 219 (1993).
[26] G. M. Hale, D. C. Dodder, E. R. Siciliano, and W. B. Wilson, *Los Alamos National Laboratory, ENDF/B-VI Evaluation, mat # 125, rev. 2, Oct. 1997; retrieved from the ENDF database at the NNDC online data service*.
[27] J. Carlson and R. Schiavilla, Reviews of Modern Physics **70**, 743 (1998).
[28] L. E. Marcucci, K. M. Nollett, R. Schiavilla, and R. B. Wiringa, Nuclear Physics A **777**, 111 (2006), arXiv:nucl-th/0402078.
[29] G. Rupak, Nuclear Physics A **678**, 405 (2000), arXiv:nucl-th/9911018.
[30] S. Ando, R. H. Cyburt, S. W. Hong, and C. H. Hyun, Phys. Rev. C **74**, 025809 (2006).
[31] D. S. Leonard, H. J. Karwowski, C. R. Brune, B. M. Fisher, and E. J. Ludwig, Phys. Rev. C **73**, 045801 (2006), arXiv:nucl-ex/0601035.
[32] U. Greife, F. Gorris, M. Junker, C. Rolfs, and D. Zahnow, Zeitschrift fur Physik A Hadrons and Nuclei **351**, 107 (1995).

[33] S. Burles, K. M. Nollett, and M. S. Turner, Astrophys. J. Lett. **552**, L1 (2001), arXiv:astro-ph/0010171.

[34] G. Fiorentini, E. Lisi, S. Sarkar, and F. L. Villante, Phys. Rev. D **58**, 063506 (1998), arXiv:astro-ph/9803177.

[35] A. Coc and E. Vangioni, Journal of Physics Conference Series **202**, 012001 (2010).

[36] LUNA Collaboration, C. Casella, H. Costantini, A. Lemut, B. Limata, R. Bonetti, C. Broggini, L. Campajola, P. Corvisiero, J. Cruz, et al., Nuclear Physics A **706**, 203 (2002).

[37] P. Descouvemont, A. Adahchour, C. Angulo, A. Coc, and E. Vangioni-Flam, Atomic Data and Nuclear Data Tables **88**, 203 (2004), arXiv:astro-ph/0407101.

[38] L. Ma, H. J. Karwowski, C. R. Brune, Z. Ayer, T. C. Black, J. C. Blackmon, E. J. Ludwig, M. Viviani, A. Kievsky, and R. Schiavilla, Phys. Rev. C **55**, 588 (1997).

[39] M. Viviani, A. Kievsky, L. E. Marcucci, S. Rosati, and R. Schiavilla, Phys. Rev. C **61**, 064001 (2000), arXiv:nucl-th/9911051.

[40] L. E. Marcucci, M. Viviani, R. Schiavilla, A. Kievsky, and S. Rosati, Phys. Rev. C **72**, 014001 (2005), arXiv:nucl-th/0502048.

[41] A. Kievsky, S. Rosati, M. Viviani, L. E. Marcucci, and L. Girlanda, Journal of Physics G Nuclear Physics **35**, 063101 (2008), arXiv:0805.4688.

[42] R. B. Wiringa, V. G. J. Stoks, and R. Schiavilla, Phys. Rev. C **51**, 38 (1995), arXiv:nucl-th/9408016.

[43] S. C. Pieper, Nuovo Cimento Rivista **31**, 709 (2008), arXiv:0711.1500.

[44] R. Esmailzadeh, G. D. Starkman, and S. Dimopoulos, Astrophys. J. **378**, 504 (1991).

[45] B. D. Fields, Ann. Rev. Nuclear & Particle Science **61**, 47 (2011).

[46] K. Hagiwara et al., Phys. Rev. D **66**, 010001 (2002).

[47] A. Serebrov, V. Varlamov, A. Kharitonov, A. Fomin, Y. Pokotilovski, P. Geltenbort, J. Butterworth, I. Krasnoschekova, M. Lasakov, R. Tal'Daev, et al., Physics Letters B **605**, 72 (2005), arXiv:nucl-ex/0408009.

[48] A. P. Serebrov, V. E. Varlamov, A. G. Kharitonov, A. K. Fomin, Y. N. Pokotilovski, P. Geltenbort, I. A. Krasnoschekova, M. S. Lasakov, R. R. Taldaev, A. V. Vassiljev, et al., Phys. Rev. C **78**, 035505 (2008), arXiv:nucl-ex/0702009.

[49] A. Pichlmaier, V. Varlamov, K. Schreckenbach, and P. Geltenbort, Physics Letters B **693**, 221 (2010).

[50] K. Nakamura et al., J. Phys. G **37**, 075021 (2010), and 2011 partial update for the 2012 edition.

[51] M. Peimbert, V. Luridiana, and A. Peimbert, Astrophys. J. **666**, 636 (2007), arXiv:astro-ph/0701580.

[52] P. Bonifacio, P. Molaro, T. Sivarani, R. Cayrel, M. Spite, F. Spite, B. Plez, J. Andersen, B. Barbuy, T. C. Beers, et al., Astron. Astrophys. **462**, 851 (2007), arXiv:astro-ph/0610245.

[53] M. Pettini, B. J. Zych, M. T. Murphy, A. Lewis, and C. C. Steidel, Mon. Not. Roy. Astron. Soc. **391**, 1499 (2008), arXiv:0805.0594.

[54] Y. I. Izotov and T. X. Thuan, Astrophys. J. Lett. **710**, L67 (2010), arXiv:1001.4440.

[55] E. Aver, K. A. Olive, and E. D. Skillman, J. Cosmo. Astropart. Phys. **3**, 43 (2011), arXiv:1012.2385.

[56] G. Steigman, Annual Review of Nuclear and Particle Science **57**, 463 (2007), arXiv:0712.1100.

[57] V. Simha and G. Steigman, J. Cosmo. Astropart. Phys.

[58] **6**, 16 (2008), arXiv:0803.3465.

[58] F. Iocco, G. Mangano, G. Miele, O. Pisanti, and P. D. Serpico, Phys. Rep. **472**, 1 (2009), arXiv:0809.0631.

[59] R. L. Porter, R. P. Bauman, G. J. Ferland, and K. B. MacAdam, Astrophys. J. Lett. **622**, L73 (2005), arXiv:astro-ph/0502224.

[60] A. M. Serenelli and S. Basu, Astrophys. J. **719**, 865 (2010), arXiv:1006.0244.

[61] M. Fumagalli, J. M. O'Meara, and J. X. Prochaska, Science **334**, 1245 (2011).

[62] D. Kirkman, D. Tytler, N. Suzuki, J. M. O'Meara, and D. Lubin, Astrophys. J. Suppl. **149**, 1 (2003), arXiv:astro-ph/0302006.

[63] G. P. Holder, K. M. Nollett, and A. van Engelen, Astrophys. J. **716**, 907 (2010), arXiv:0907.3919.

[64] T. M. Bania, R. T. Rood, and D. S. Balser, Space Sci. Rev. **130**, 53 (2007).

[65] C. J. Hogan, Astrophys. J. Lett. **441**, L17 (1995), arXiv:astro-ph/9407038.

[66] F. Spite and M. Spite, Astron. Astrophys. **115**, 357 (1982).

[67] M. Asplund, D. L. Lambert, P. E. Nissen, F. Primas, and V. V. Smith, Astrophys. J. **644**, 229 (2006), arXiv:astro-ph/0510636.

[68] S. Bashinsky and U. Seljak, Phys. Rev. D **69**, 083002 (2004), arXiv:astro-ph/0310198.

[69] E. Shirokoff, C. L. Reichardt, L. Shaw, M. Millea, P. A. R. Ade, K. A. Aird, B. A. Benson, L. E. Bleem, J. E. Carlstrom, C. L. Chang, et al., Astrophys. J. **736**, 61 (2011), arXiv:1012.4788.

[70] P. Ahrendt, *The multivariate gaussian probability distribution* (2005), URL http://www2.imm.dtu.dk/pubdb/p.php?3312.

[71] F. Hoyle and R. J. Tayler, Nature (London) **203**, 1108 (1964).

[72] F. X. Timmes, S. E. Woosley, and T. A. Weaver, Astrophys. J. Suppl. **98**, 617 (1995), arXiv:astro-ph/9411003.

[73] M. Asplund, N. Grevesse, A. J. Sauval, and P. Scott, Ann. Rev. Astron. Astrophys. **47**, 481 (2009), arXiv:0909.0948.

[74] B. E. J. Pagel, Phys. Rep. **333**, 433 (2000).

[75] M. Archidiacono, E. Calabrese, and A. Melchiorri, ArXiv e-prints (2011), arXiv:1109.2767.

[76] A. X. Gonzalez-Morales, R. Poltis, B. D. Sherwin, and L. Verde, ArXiv e-prints (2011), arXiv:1106.5052.

[77] J. Hamann, ArXiv e-prints (2011), arXiv:1110.4271.

[78] G. Mangano, G. Miele, S. Pastor, T. Pinto, O. Pisanti, and P. D. Serpico, Nuclear Physics B **729**, 221 (2005), arXiv:hep-ph/0506164.

[79] Even within the standard model, $N_{eff} \neq 3$ after the temperature drops below the electron rest mass. At that time, all electron-positron pairs annihilate, transferring their energy mainly into the photon bath. A small fraction of annihilations produce neutrino pairs that fail to thermalize, contributing energy equivalent to 0.046 of a relativistic species to the subsequent evolution [78]. In the CMB literature, N_{eff} within the standard model is generally taken to be 3.046, but since pair annihilation occurs during BBN, most BBN work refers to the standard-model case as $N_{eff} = 3$. We report results in terms of N_{eff} at late times, so that the standard model has $N_{eff} = 3.046$.

Data	CMB+Y_{p}	CMB+BBN+Y_{p}	CMB+BBN+Y_{p}+D/H	BBN+Y_{p}+D/H
Aver et al	3.82 ± 0.74	3.84 ± 0.24	3.87 ± 0.24	3.85 ± 0.26
Izotov & Thuan	3.83 ± 0.75	3.77 ± 0.36	3.83 ± 0.35	3.82 ± 0.45
Peimbert et al	4.02 ± 0.79	3.18 ± 0.21	3.22 ± 0.19	3.13 ± 0.21
CMB only			3.4 ± 1.0	
CMB+$0.22 < Y_{\mathrm{p}} < Y_{\mathrm{proto}}$			3.87 ± 0.81	
CMB+BBN			3.89 ± 0.60	
CMB+BBN+D/H			3.90 ± 0.44	

TABLE I: Constraints on N_{eff} from various combinations of data sets. The first three rows of results use three different precise determinations of Y_{p}, while the corresponding columns show different combinations of these Y_{p} measurements with CMB data, BBN theory (including errors on reaction rates), and D/H abundance measurements. The lower set of results do not use these precise Y_{p} measurements.